J Mater Sci (2012) 47:4028–4035
DOI 10.1007/s10853-012-6256-y

Structure and properties of CaF_2–B_2O_3 glasses

H. Doweidar · G. El-Damrawi · M. Abdelghany

Received: 3 October 2011 / Accepted: 5 January 2012 / Published online: 20 January 2012

Abstract FTIR spectroscopy has been employed to investigate the structure of CaF_2–B_2O_3 glasses. It is proposed that CaF_2 partially modifies the borate network forming $Ca^{2+}_{1/2}[BO_{3/2}F]^-$ units. The rest of CaF_2 is assumed to build an amorphous network formed of CaF_4 tetrahedra. Analysis of density and molar volume revealed that the volume of CaF_4 tetrahedron in the studied glasses is slightly greater than that in the crystalline form. Data of density, molar volume, and electric conductivity have been correlated with the glass structure. As far as the authors know, CaF_2–B_2O_3 glasses are investigated for the first time.

Introduction

Since publishing of the pioneer work of Gressler and Shelby on PbF_2–B_2O_3 [1] and PbO–PbF_2–B_2O_3 glasses [2], the structure and properties of borate glasses containing F^- ions have been the subject of growing interest. These types of glass show a wide variety of physical properties and are characterized with their anionic conduction. They are classified among the well-known fast ionic conductors. However, there is a main controversy about the role of F^- ions.

X-ray photoelectron spectroscopy (XPS) of F (1s) in $(70-x)PbO{\cdot}xPbF_2{\cdot}30B_2O_3$ glasses [3] showed two peaks. A peak is assigned to F^- ions in Pb–F–Pb clusters (free F^-) and the other is related to non-bridging fluorine atoms in the borate network ($B–F^-…Pb^{2+}$). Gopalakrishnan et al. [4] indicated that in $xPbF_2{\cdot}(1-x)B_2O_3$ glasses fluorine is incorporated predominantly as B–O–F at high B_2O_3 content, whereas it forms Pb–O–F bonds at high PbF_2 content.

Chowdari and Rong [5] indicated that upon increasing the fluorine content in fluorinated lithium borate glasses, the number of four-coordinated boron atoms increases and the asymmetric BO_3 groups with non-bridging oxygen atoms decreases. These results are assumed as an evidence that fluorine participates in the boron–oxygen network. X-ray photoelectron spectra of F (1s) show two peaks. One of them is related to fluoride ions associated with lithium ions forming Li–F bond and the other is assigned to non-bridging fluorine atoms ($B–F…Li^+$). The latter may contribute to the formation of BO_3F and BO_2F_2 units with non-bridging bonds. Formation of these structural units was confirmed by NMR investigations on NaF–Na_2O–B_2O_3 glasses [6, 7] with an estimation of the highest probability for the formation of BO_3F units. Suresh and Chandramouli [8] discussed structural variations in $(30-x)Na_2O{\cdot}xNaF{\cdot}50B_2O_3{\cdot}20Bi_2O_3$ glasses, with increasing the NaF content, on the basis of the formation of BO_3F and BO_2F_2 units. Both structural units are also considered to be formed in Li_2O–SrO–SrF_2–B_2O_3 glasses [9].

Alkali fluoroborate glasses with alkali fluoride content up to 45 mol% LiF or 55 mol% NaF or KF showed composition-properties trends similar to that observed for alkali borate glasses. To explain the differences in behavior between the alkali fluoroborate glasses and the corresponding alkali borate glasses Shelby and Baker [10] proposed a structural model based on the replacement of BO_4 tetrahedra by BO_3F tetrahedra. The model is based on NMR investigations in sodium fluoroborate glasses [11, 12].

Formation of some different types of fluoroborate units like BO_2F (or BOF_2) is assumed in B_2O_3–xLi_2O–$yLiX$ (X = F, Cl, Br, and I) [13]. The B–F in these units is a

H. Doweidar (✉) · G. El-Damrawi · M. Abdelghany
Glass Research Group, Physics Department, Faculty of Science, Mansoura University, El Mansura 35516, Egypt
e-mail: hdoweidar@mans.edu.eg

terminal one and the bond can be described as a non-bridging bond.

Changes in the electric conductivity with fluorine content in MeF_2–$Na_2B_4O_7$ glasses (Me = Mg, Ca, Sr, and Ba) have been attributed to formation of a number of structural units. Sokolov et al. [14] assumed the structure of those glasses is built up of nonpolar $BO_{3/2}$ units and various polar groupings such as $Na^+[BO_{4/2}]^-$, $Na^+[F^-BO_{3/2}]^-$, $Me_{1/2}[BO_{4/2}]^-$, $Me_{1/2}[F^-BO_{3/2}]^-$, $[MeF_{4/2}]$, and $[MeF_{6/3}]$. Among these units, $Na^+[BO_{4/2}]^-$ and $Na^+[F^-BO_{3/2}]^-$ are the most probably formed species [15, 16]. The negative charge on the regular $[BO_{4/2}]$ tetrahedron has a uniform distribution, whereas it is localized at F^- ion in the distorted $[F^-BO_{3/2}]$ tetrahedron.

Another type of structural units is proposed by Sokolov et al. [17]. They proposed formation of $Na^+[F^-BO_{4/2}]^-$ oxyfluoride structural units in NaF–Na_2O–B_2O_3 and NaF–B_2O_3 glasses. Although these units are electrically unbalanced, it has been indicated that fluorine ions are not consumed only in these units but they can also be bound to Na^+ ions in $F^-\ldots Na^+[F^-BO_{4/2}]$ structural units.

Hager and El-Hofy [18] used IR spectroscopy to study the structure of $(70-x)B_2O_3{\cdot}30BaF_2{\cdot}xLiX$ glasses, where X = F, Cl and Br. They concluded that these glasses mainly contain BO_3, BO_2F triangles and BO_4, and BOF_3 tetrahedra. Formation of BO_2F triangles is, however, ruled out in NaF–Na_2O–B_2O_3 glasses [7, 19].

Multi nuclei ^7Li, ^{11}B, ^{19}F, and ^{207}Pb single- and double-resonance NMR experiments indicated that units such as $BO_{4/2}{}^-$, $BO_{3/2}F^-$ are expected to form in $50B_2O_3$–$(50-x)$ PbO–xLiF glasses ($10 \leq x \leq 40$ mol%) [20]. Furthermore, formation of $BO_{2/2}F$ units is also possible. The ^{19}F–^7Li dipole–dipole coupling of $50B_2O_3$–10PbO–40LiF glass is weaker than that of crystalline LiF. This result stands against considering formation of large LiF-like domain in these glasses. At the same time, it agrees well with the assumption that LiF contributes in the formation of the above structural units. The authors also assumed a random distribution of F^- ions with respect to Pb^{2+} ions without preferential formation of PbF_2-like domains.

Ayta et al. [21] investigated Li_2O–B_2O_3–Al_2O_3 glasses containing CaF_2. The compositions they investigated are $[(50Li_2O–45B_2O_3–5Al_2O_3)$ (mol%) + $xCaF_2$ (wt%)], with $0 \leq x \leq 50$. Thermoluminescence glow curves presented an evidence for CaF_2-crystal formation in these glasses.

The above literature survey reveals that a little work has been carried out on alkaline earth oxyfluoro borate glasses. In addition, as far as the authors know, no work has yet been done on binary alkaline earth fluoroborate glasses. In this article, the structure of CaF_2–B_2O_3 glasses would be explored by means of infrared spectroscopy. Density and electric conduction parameters would be correlated with the glass structure.

Experimental

Glasses having the formula $xCaF_2$–$(100-x)B_2O_3$ ($30 \leq x \leq 45$ mol%) were prepared from reagent grade chemicals. Boric acid H_3BO_3 and calcium fluoride CaF_2 were used as sources for the corresponding oxides. The glasses were prepared under normal atmospheric conditions by melting the mixture of raw materials in porcelain crucibles in an electric furnace for about 30 min at a temperature ranged between 800 and 900 °C depending on the composition. To get a homogeneous glass the melt was swirled from time to time. After the melt becomes homogeneous, it was poured on steel plates and then pressed by a ceramic plate to obtain glass disks at room temperature. The disks were used for the measurement of the electrical conductivity. Samples prepared by pouring the melt onto steel plates without pressing were used for the density measurement. All the obtained samples were visually homogeneous and transparent. The glass samples were kept in desiccators until required.

The amorphous nature of the samples was confirmed by X-ray diffraction investigations. A Bruker D8 Advance powder XRD was used. It is fitted with a Vantech Super Speed position sensitive detector and a Cu K_α X-ray tube with a Gobel Mirror. Measurements were made over the range 4°–130° in 2-theta. X-ray diffraction patterns of all the studied glasses show only broad humps typical of amorphous materials.

The density (D) of glasses was determined at room temperature using the Archimedes method with xylene as an immersion fluid. At least, three samples of each glass were used to determine the density. Density values are precise to ± 0.02 g/cm^3.

For measuring the dc resistivity, polished disks with a thickness of about 1 mm were coated with silver paste to serve as electrodes. The resistance was measured using a type TM14 insulation tester (Levell Electronics Ltd, UK) with a range of 10^3–10^{13} Ω. Three samples of each glass were used to measure the resistance. The experimental error in determining the activation energy for conduction is estimated to be less than 0.025 eV, whereas the relative error in the conductivity is expected to be ±5%.

The infrared spectra of the glasses were recorded at room temperature using the KBr disk technique. A Mattson 5000 FTIR spectrometer was used to obtain the spectra in the wavenumber range between 400 and 2000 cm^{-1} with a resolution of 2 cm^{-1}. At least two spectra for each sample were recorded. Infrared spectra were corrected for the dark current noises and background using the two-point baseline correction. After correction, the IR spectra were analyzed using the deconvolution method. More details about this method are reported elsewhere [22, 23].

Results

Figure 1 shows normalized IR spectra of the investigated $x\mathrm{CaF_2}\cdot(100-x)\mathrm{B_2O_3}$ glasses ($30 \leq x \leq 45$ mol%). There are two main strong absorption bands in the regions 800–1200 and 1200–1800 $\mathrm{cm^{-1}}$. In addition, a small absorption band appears around 700 $\mathrm{cm^{-1}}$ in all the spectra. There is mostly no change of band centers with composition of glass.

Figure 2 shows the dependence of density (D) and molar volume (V_m) on the $\mathrm{CaF_2}$ content in $\mathrm{CaF_2}$–$\mathrm{B_2O_3}$ glasses. There is a linear increase in the density, whereas a linear decrease is observed in V_m. The increase in D reveals that the developed structural units, by replacing $\mathrm{CaF_2}$ for $\mathrm{B_2O_3}$, are denser than the $\mathrm{BO_3}$ units. On the other hand, the decrease in V_m indicates that the resultant volume of the formed structural units is smaller than that of the start glass ($30\mathrm{CaF_2}\cdot70\mathrm{B_2O_3}$).

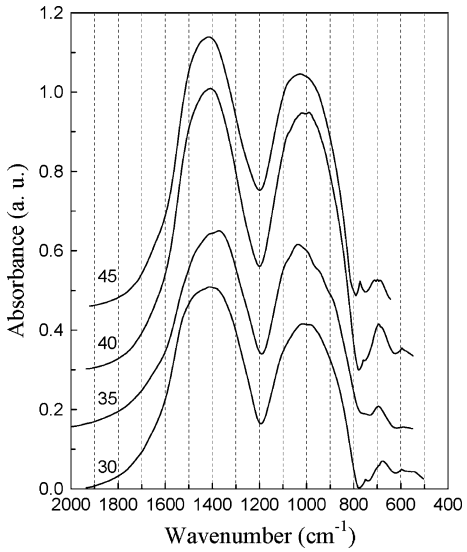

Fig. 1 Infrared spectra of the investigated $x\mathrm{CaF_2}$–$(100-x)\mathrm{B_2O_3}$ glasses. Values of x are given at the plots

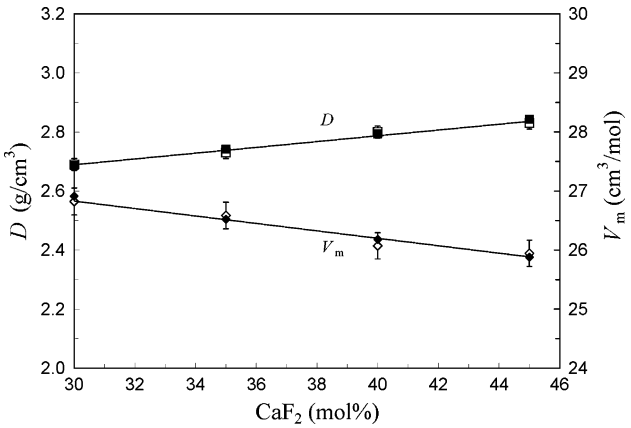

Fig. 2 Dependence of the density D and molar volume V_m of the studied glasses on the $\mathrm{CaF_2}$ content. *Open symbols* represent the experimental values and the *closed ones* are calculated. Eq. 7 and the experimental D data were used to get experimental V_m values. Estimated error limit in the latter is about 0.9%. Eqs. 6 and 8 are used to get the calculated D and V_m values. *Lines* are fitting plots of the data

All investigated glasses show a linear dependence of the logarithm of conductivity (log σ) on the reciprocal of absolute temperature ($1/T$), Fig. 3. This a feature of ionic conduction process that can be described by the Arrhenius relation

$$\sigma = \sigma_0 \exp(-E/kT) \quad (1)$$

In this relation σ_0 is a constant that depends on the glass composition and its thermal history, E is the activation energy for the conduction process, k is the Boltzmann's constant and T is the absolute temperature.

Discussion

Infrared spectra

The IR spectra shown in Fig. 1 can be described based on the assignment of those of borate glasses modified with oxides. The absorption of borate glasses in the region $\sim$850–1100 $\mathrm{cm^{-1}}$ is related to B–O bond stretching vibration of $\mathrm{BO_4}$ tetrahedra and the absorption peaks in the region $\sim$1150–1600 $\mathrm{cm^{-1}}$ are attributed to stretches of B–O in $\mathrm{BO_3}$ units [24–28]. Formation of $\mathrm{BO_4}$ tetrahedra in oxide glasses results from modifying the borate matrix with the modifier oxide. In this study, where there is no modifier oxide, $\mathrm{B_2O_3}$ is modified only with $\mathrm{CaF_2}$. The presented literature survey on the structure of fluorborate glasses reveals that, among various structural units that may form in such glasses, $[\mathrm{BO_{3/2}F}]^-$ distorted tetrahedra are suggested to be the single [10–12] or the most probably formed

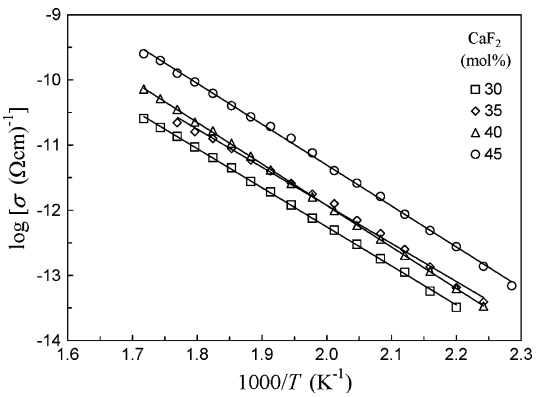

Fig. 3 Logarithm of the electrical conductivity (log σ) of the investigated $x\mathrm{CaF_2}$–$(100-x)\mathrm{B_2O_3}$ glasses on the reciprocal of absolute temperature ($1/T$). *Lines* are fitting plots of the data

[6, 7, 15, 20] oxyfluoro borate species. In this study, four-coordinated boron atoms are assumed to be in the form of BO_3F (B_4 units) and the absorption in the region $\sim$800–1200 cm^{-1} might be correlated with their vibrations.

IR spectra of various glasses [27–29] could be quantitatively analyzed by deconvoluting the absorption peaks into their individual component bands. Figure 4 shows, as an example, the deconvolution of IR spectrum of the glass $45CaF_2{\cdot}65B_2O_3$.

Figure 5 shows a slight increase in the fraction N_4 of four-coordinated boron atoms with increasing the CaF_2 content. The fraction N_4 of four-coordinated boron atoms can be calculated from the area under the component bands since the area is related to the concentration of the borate groups originating it. N_4 is defined as the ratio of [concentration of B_4 units/concentration of (BO_3 + B_4) units]. The increase in N_4 indicates that BO_3 units convert successively into B_4 units. The values obtained of N_4 (Fig. 5) agree quite well with those found for $CaO–B_2O_3$ glasses by analyzing the IR spectra [30] and pulsed neutron diffraction and molecular dynamics studies [31]. N_4 values are nearly the same at similar concentration of CaF_2 and CaO. Because of the comparable masses and nearly equal radii of fluorine and oxygen, drastic changes are not expected to be observed in the mid-IR spectra when introducing fluorine at the expanse of oxygen [32].

N_4 values obtained from the equation of fitting line in Fig. 5

$$N_4 = 0.0035x + 0.286 \quad (2)$$

can be employed to obtain the concentration of various structural units in the studied glasses. The quantity $(B_2O_3)_4$ (mol%) of B_2O_3 converted into B_4 units, is given as

$$(B_2O_3)_4 = N_4(B_2O_3) \quad (3)$$

where (B_2O_3) is the concentration of B_2O_3 in the glass (mol%). The quantity $(B_2O_3)_4$ equals to the quantity, CaF_2(m), of CaF_2 that modifies B_2O_3 to B_4 units at a rate of two units per CaF_2 molecule. The rest of B_2O_3 that remains as BO_3 units $(B_2O_3)_3$, can be given by

$$(B_2O_3)_3 = B_2O_3 - N_4(B_2O_3). \quad (4)$$

In addition, the quantity CaF_2(f), of CaF_2 that enters the structure as network former is given as

$$CaF_2(f) = CaF_2 - N_4(B_2O_3). \quad (5)$$

In crystalline CaF_2, Ca is tetrahedrally coordinated with F^- ions [33]. It is, therefore assumed that CaF_2(f) may be present in the structure in the form of CaF_4 tetrahedra. Figure 6 shows X-ray diffraction patterns of crystalline CaF_2 and $CaF_2–B_2O_3$ glasses having 30, 40, and 45 mol% CaF_2. There is coincidence of the 2θ values of the sharp peaks in the spectrum of crystalline CaF_2 with the centers of the broad humps in the diffraction patterns of the glasses. This suggests that CaF_2 is present in its amorphous form in the studied glasses. In Fig. 7 is shown the dependence on CaF_2 content of $(B_2O_3)_4$, $(B_2O_3)_3$, and

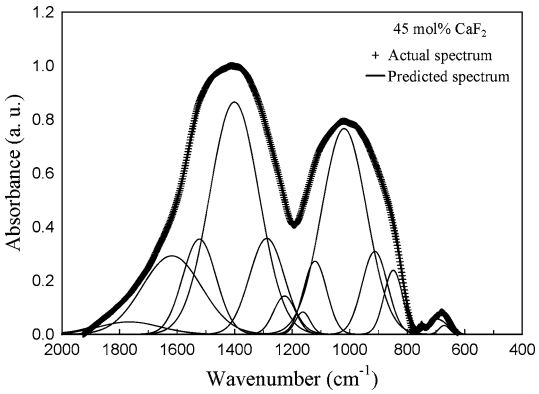

Fig. 4 Deconvolution of the infrared spectrum of the glass $45CaF_2{\cdot}55B_2O_3$

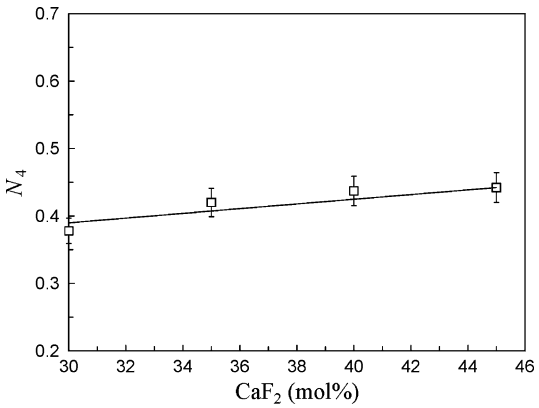

Fig. 5 Fraction of four-coordinated boron N_4 as a function of the CaF_2 content in $xCaF_2$–$(100-x)B_2O_3$ glasses. Error limit for N_4 values is estimated as ±5%. *Line* is a fitting plot of the data

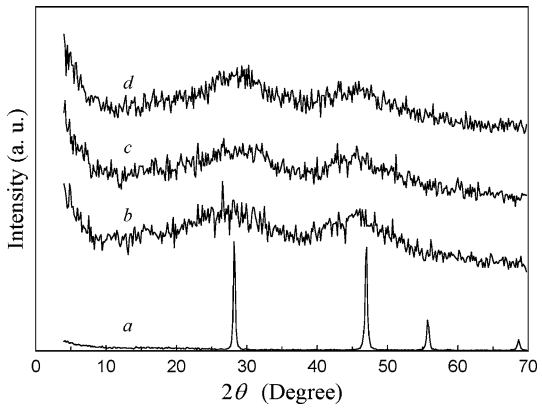

Fig. 6 XRD patterns of crystalline CaF_2 (plot *a*) and $CaF_2–B_2O_3$ glasses having 30, 40, and 45 mol% CaF_2 (plots *b*, *c*, and *d*, respectively)

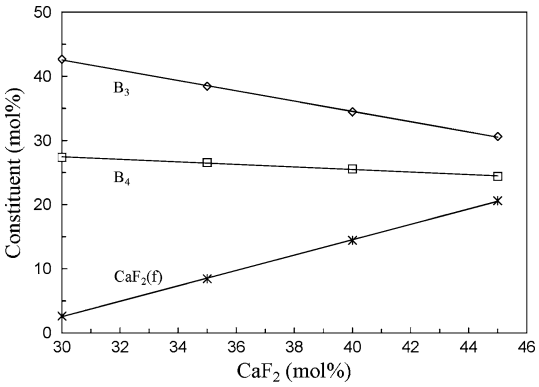

Fig. 7 Dependence on the CaF_2 content of B_3 (*triangular* boron $(B_2O_3)_3$), B_4 (*tetrahedral* boron $(B_2O_3)_4$) and CaF_2(f) in the studied glasses. Concentration of CaF_2(m) equals to that of B_4. *Lines* are fitting plots of the data

CaF_2(f), as obtained from Eqs. 3–5, respectively. There is a linear decrease in both $(B_2O_3)_3$ and $(B_2O_3)_4$ while CaF_2(f) increases linearly overall the CaF_2 content. The decrease in both of $(B_2O_3)_3$ and $(B_2O_3)_4$ can mainly be attributed to the low rate of N_4 increase (Fig. 5) and partially to the decrease in the content of B_2O_3 when increasing that of CaF_2. The change in the content of $(B_2O_3)_4$ and CaF_2(f) indicates that CaF_2 tends preferentially to form its own matrix rather than modifying the borate network.

Density and molar volume

The information obtained from the IR spectra can be used to calculate D and V_m. As previously indicated [34], the density of a glass can be expressed as

$$D = \frac{\sum_u n_u M_u}{\sum_u n_u V_u} \tag{6}$$

where n_u is the number of the structural unit u per mole of glass. M_u and V_u are, respectively, the mass and volume of the structural unit.

As revealed from the IR spectra, the investigated glasses contain different structural units. These are symmetric BO_3 units, B_4 units and the network former units of CaF_2. On the basis of Eq. 6 the density can then be expressed as

$$D = (n_4M_4 + n_3M_3 + n_fM_f)/(n_4V_4 + n_3V_3 + n_fV_f). \tag{7}$$

Here n_4, n_3 and n_f represent, respectively, the number (per mole of glass) of B_4, BO_3, and the network former units of CaF_2 (CaF_4 tetrahedra). M_f and V_f are, respectively, the mass and volume of the former units, CaF_2(f), of CaF_2. The masses are taken as $M_4 = (B + 1.5O + F + 0.5Ca)$, $M_3 = (B + 1.5O)$ and $M_f = (Ca + 2F)$. To calculate n_4, n_3 and n_f Eq. 1 would be used, where x is the CaF_2 content in the glass expressed in mol%. N_4 values obtained from Eq. 1 can be used in Eqs. 3–5 to get n_3, n_4, and n_f as

$$n_4 = 2N_4(B_2O_3)N_A/100, \tag{3a}$$

$$n_3 = 2[B_2O_3 - N_4(B_2O_3)]N_A/100 \tag{4a}$$

and

$$n_f = [CaF_2 - N_4(B_2O_3)]N_A/100 \tag{5a}$$

where N_A is Avogadro's number. The factor 2 appears in Eqs. 3a and 4a because each CaF_2 converts two BO_3 units into two B_4 units and each B_2O_3 molecule produces two BO_3 units.

The density of vitreous B_2O_3 is 1.838 g/cm^3 [35] and thus a value of $V_3 = 3.14 \times 10^{-23}$ cm^3 could be estimated. This value of V_3 has been found mostly the same in various borate glasses, such as $PbO–B_2O_3$ [36], $Al_2O_3–PbO–B_2O_3$ [29] and $Na_2O–Al_2O_3–B_2O_3$ [37]. In the light of these findings, it is assumed that V_3 has the same value in $CaF_2–B_2O_3$ glasses.

To get the volumes V_4 and V_f (of B_4 and the network former units of CaF_2, respectively) it is adequate to start by analyzing the molar volume. The latter is given as

$$V_m = M/D \tag{8}$$

where M is the relative molecular mass of glass. In terms of the concentration and volume of structural units it can be expressed as

$$V_m = (n_3V_3 + n_4V_4 + n_fV_f)N_A. \tag{9}$$

Taking $V_3 = 3.14 \times 10^{-23}$ cm^3, Eq. 9 can be solved simultaneously for two V_m values close to each other to get V_4 and V_f. In the seek of getting reliable values, the equation of fitting line for the experimental data of V_m in Fig. 2 would be used. This equation gives the molar volume as a function of the concentration x of CaF_2 (mol%) as

$$V_m = -0.063x + 28.719. \tag{10}$$

Figure 8 shows the dependence of the volume of B_4 and CaF_2(f) on the CaF_2 content. It is shown that V_4 is mostly constant whereas V_f decreases linearly with increasing the content of CaF_2. The decrease in V_f reaches about 7% at 44 mol% CaF_2. The average values of V_4 and V_f are 3.10×10^{-23} and 4.32×10^{-23} cm^3, respectively. These values, together with that of V_3, can be used, respectively, in Eqs. 7 and 9 to calculate both D and V_m. Reasonable agreement between calculated and experimental data could be obtained. However, a better agreement (Fig. 2) could be attained by means of $V_3 = 3.12 \times 10^{-23}$, $V_4 = 3.1 \times 10^{-23}$ and $V_f = 4.25 \times 10^{-23}$ cm^3. It is worthy to indicate that the density of CaF_2 is 3.18 g/cm^3 [38] that gives $V_f = 4.077 \times 10^{-23}$ cm^3. This reveals that the mean value

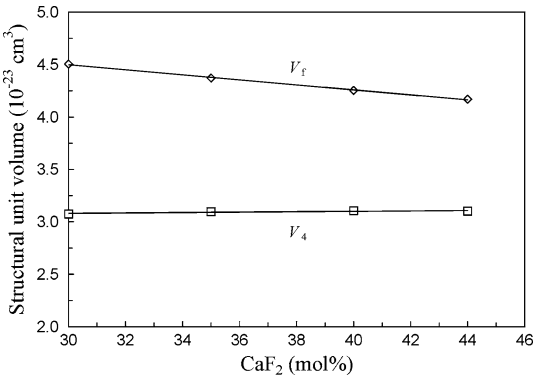

Fig. 8 The volume V_4 (of $Ca^{2+}_{1/2}[BO_{3/2}F]^-$unit) and V_f (of CaF_2(f) unit) as a function of the CaF_2 content in the investigated $xCaF_2$–$(100-x)B_2O_3$ glasses. *Lines* are fitting plots of the data

of V_f in the amorphous form is about 1.04 times that in the crystalline form. This result is consistent with the conclusions of Ayta et al. [21]. Thermoluminescence glow curves presented an evidence for CaF_2-crystal formation in [$(50Li_2O–45B_2O_3–5Al_2O_3)$ (mol%) + $xCaF_2$ (wt%)] glasses, with $0 \leq x \leq 50$. The decrease in V_f with increasing CaF_2 content (Fig. 8) can be attributed to competition of the former CaF_2(f) units to occupy space among other units in the glass matrix. The decrease in V_f with increasing the CaF_2 content (Fig. 8) reveals that CaF_4 units tend to reach their volume in the pure crystalline form.

The difference observed between the volume of CaF_4 units in the investigated glasses and in crystalline CaF_2 is consistent with various studies. Watanabe et al. [39] investigated $CaO–CaF_2–SiO_2$ glasses ($5 \leq CaF_2 \leq 25$ mol%) using ^{19}F NMR. They reported that Ca–F clusters are formed and the cluster size, as well as the Ca–F distance, increase with increasing the CaF_2 content. Brauer et al. [40] used ^{19}F and ^{29}Si MAS NMR to investigate $SiO_2–P_2O_5–Na_2O–CaO–CaF_2$ glasses ($0 \leq CaF_2 \leq 32.7$ mol%). It is deduced that fluorine does not form Si–F bonds. Instead, fluorine forms mixed sodium–calcium species. However, by increasing the CaF_2 content, fluorine preferentially complexes Ca^{2+} rather than Na^+ ions. They attributed the higher chemical shift of F–Ca(n), compared with F–Ca(4) or F–Ca(3) in crystalline species, to the slightly longer Ca–F distance in the amorphous form [41]. Recently, an investigation on the density of $SiO_2–P_2O_5–Na_2O–CaO–CaF_2$ glasses ($0 \leq CaF_2 \leq 25.54$ mol%) revealed that CaF_2 enters the structure as CaF_4 tetrahedra [42]. The mean volume found for CaF_4 unit (4.142×10^{-23} cm^3) is close of that in the present work.

The density of the studied glasses can be calculated by using the predicted volumes in Eq. 7. Figure 2 shows that the calculated density and molar volume agree well with the experimental data, which supports the structural view of the studied glasses.

Electric conduction

Figure 9 shows that there is a small change in both E and $\log\sigma_{523}$ (log conductivity at 523 K) when changing the CaF_2 content. Between 30 and 45 mol% CaF_2 there is an increase of about one order in $\log\sigma_{523}$. These features are greatly different from those of $PbF_2–B_2O_3$ glasses [1], where a fast increase in $\log\sigma_{473}$ (about six orders) takes place between 35 and 60 mol% PbF_2. The marked change in the conductivity of $PbF_2–B_2O_3$ glasses is attributed to the ease of transport of F^- ions as charge carriers [1]. The small increase in $\log\sigma_{523}$ and the activation energy (Fig. 9) can be taken as a basis to rule out the role of F^- ions as the major type of charge carriers in the studied $CaF_2–B_2O_3$ glasses. It is therefore to assume that the electric conduction in these glasses is mainly due to transport of Ca^{2+} ions rather than F^- ions.

In Fig. 7 is shown that the content of CaF_2(f) (the former CaF_2) increases whereas that of B_4 (the modifier CaF_2) slightly decreases with increasing the concentration of CaF_2. It can be indicated that the concentration of these components expressed as number/cm^3 changes in the same manner. The increase in conductivity with increasing CaF_2 content (Fig. 9) leads likely to consider Ca^{2+} ions in CaF_2(f) being the main charge carriers in the studied $CaF_2–B_2O_3$ glasses. Because of the small increase in conductivity it can be deduced that the mobility has a pronounced effect. The conductivity is generally given by [43] as

$$\sigma = nq\mu \tag{11}$$

where n is the concentration of mobile ions expressed as (number/cm^3), q is the ionic charge, and μ is the mobility of the charge carrier. It must be noted that the concentration n of mobile ions is just a fraction of ionic species that is assigned as charge carriers. This fraction is usually unknown and therefore it is not possible to determine the

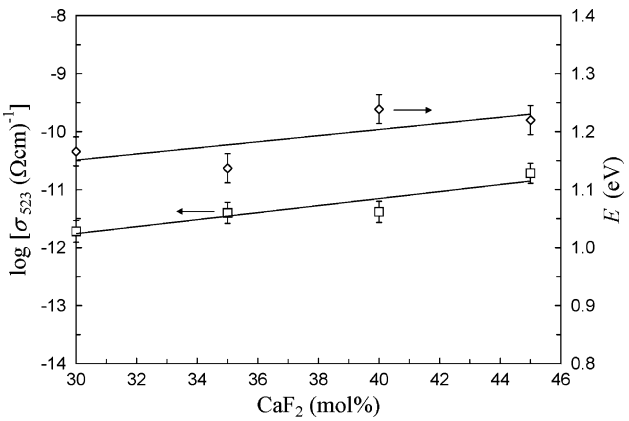

Fig. 9 Dependence of both the logarithm of conductivity at 523 K and activation energy for electric conduction on the CaF_2 content in the studied glasses. *Lines* are guide for the eyes

mobility of charge carriers from Eq. 11. To get an idea about the change of mobility with composition of glass it can be assumed that all Ca^{2+} ions in CaF_2(f) are mobile ions. Thus, Eq. 11 can be used to calculate the mean mobility ($\overline{\mu}$) of Ca^{2+} ions. Figure 10 shows that, in spite of the marked increase (>four times) in the total concentration n_{Ca} of Ca^{2+} ions in CaF_2(f), the logarithm of $\overline{\mu}$ decreases with increasing the CaF_2 content. The decrease in $\overline{\mu}$ can be correlated with the decrease in the molar volume (Fig. 2) and thus the free volume of glass when the CaF_2 content increases (Fig. 11). The decrease in free volume can also be the reason that E does not change when changing the CaF_2 content (Fig. 9).

In addition to the effect of decreasing free volume, another factor may contribute to the low conductivity and its limited increase between 30 and 45 mol% CaF_2. This is the nature of binding of Ca^{2+} ions in the studied glasses. These ions are bound to F^- ions either in $[F^-BO_{3/2}]$, where the negative charge is localized at F^- ion in the distorted

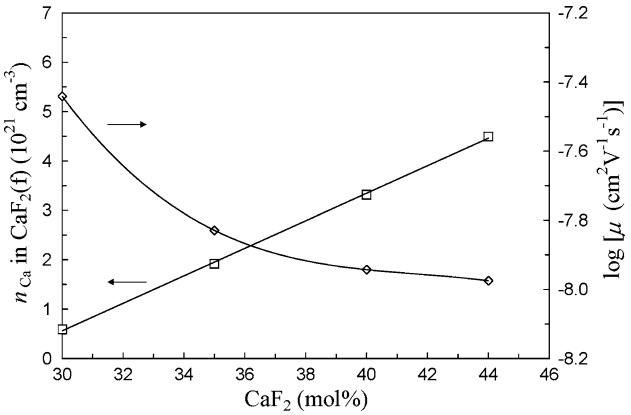

Fig. 10 Concentration n_{Ca} of Ca^{2+} ions in CaF_2(f) and the logarithm of mean mobility of Ca^{2+} ion (log $\overline{\mu}$) in dependence of the CaF_2 content in the investigated $xCaF_2$–$(100-x)B_2O_3$ glasses. *Lines* are fitting plots of the data

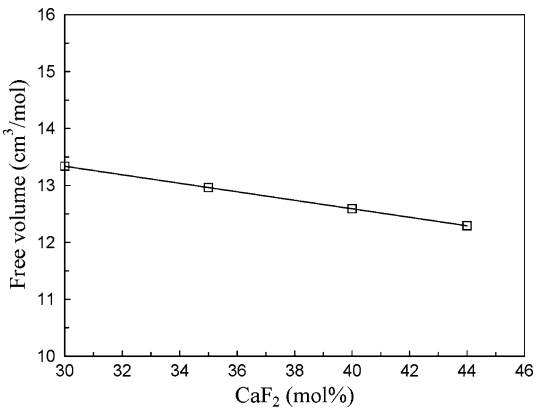

Fig. 11 Change of the free volume of $xCaF_2$–$(100-x)B_2O_3$ glasses with composition. *Lines* are fitting plots of the data

$[F^-BO_{3/2}]$ tetrahedron [15, 16], or in CaF_4 tetrahedra. A reduction in the mobility of Na^+ ions in xNa_2O–$y(NaF)_2$–$0.64B_2O_3$ and $y(NaF)_2$–$(1-y)B_2O_3$ glasses were reported upon increasing the concentration of fluoride ions. The effect is attributed to a stronger interaction between Na^+ ions and F^- ions, compared to that with O^{2-} ions [32]. Similar results were obtained by Jain et al. [44] upon replacing 1% of total oxygen concentration by fluorine in $0.35(Li, Na)_2O{\cdot}0.65B_2O_3$ glasses. In this study, an increase in the CaF_2 content means an increase F/O ratio and this leads to a decrease in the mobility of Ca^{2+} ions.

Conclusion

IR absorption in the region ~850–1200 cm^{-1} is assumed to be related to stretching vibrations of $Ca^{2+}_{1/2}[BO_{3/2}F]^-$ units. A part of CaF_2 is incorporated in the borate network to form these units. The rest of CaF_2 forms its own matrix, presumably in the form of CaF_4 tetrahedra. Calculated density agrees well with the experimental density. Calculated density has been obtained by considering that the studied CaF_2–B_2O_3 glasses may contain BO_3, $Ca^{2+}_{1/2}[BO_{3/2}F]^-$and CaF_2(f) units. Calculated volume of the latter has mostly the same value as in the crystalline CaF_2. Ca^{2+} ions are the main charge carriers in the studied glasses. A limited increase in conductivity is related to the decrease in the mean mobility, in spite of the increase in the total concentration of Ca^{2+} ions. The decrease in the mean mobility is attributed to a decrease in the free volume with increasing the CaF_2 content.

References

1. Gressler CA, Shelby JE (1988) J Appl Phys 64:4450
2. Gressler CA, Shelby JE (1989) J Appl Phys 66:1127
3. Wang Y, Osaka A, Miura Y (1989) J Mat Sci Lett 8:421
4. Gopalakrishnan R, Tan KL, Chowdari BVR, Vijay AR (1994) J Phys D Appl Phys 27:2612
5. Chowdari BVR, Rong Z (1995) Solid State Ionics 78:133
6. Kline D, Bray PJ (1966) Phys Chem Glasses 7:41
7. Jager Chr, Haubenreisser U (1985) Phys Chem Glasses 26:152
8. Suresh S, Chandramouli V (2004) Indian J Pure Appl Phys 42:560
9. Huang Y, Jang K, Wang X, Jiang C (2008) J Rare Earths 26:490
10. Shelby JE, Baker LD (1998) Phys Chem Glasses 39:23
11. Shelby JE, Downiel K (1989) Phys Chem Glasses 30:151
12. Shelby JE, Ortolanor L (1990) Phys Chem Glasses 31:25
13. Souto S, Massot M, Balkanski M, Royer D (1999) Mater Sci Eng B 64:33
14. Sokolov IA, Naraev VN, Nosakin AN, Pronkin AA (2000) Glass Phys Chem 26:383
15. Pronkin AA, Naraev VN, Eliseev SYu (1988) Fiz Khim Stekla 14:926 cited in [14]

16. Pronkin AA, Naraev VN, Tsoi TB, Eliseev SYu (1992) Sov J Glass Phys Chem Engl Transl 18:304 cited in [14]
17. Sokolov IA, Naraev VN, Nosakin AN, Pronkin AA (2000) Glass Phys Chem 26:584
18. Hager IZ, ElHofy M (2003) Phys Stat Sol A 198:7
19. Maya L (1977) J Am Ceram Soc 60:323
20. Cattaneo AS, Lima RP, Tambelli CE, Magon CJ, Mastelaro VR, Garcia A, de Souza JE, de Camargo ASS, de Araujo CC, Schneider JF, Donoso JP, Eckert H (2008) J Phys Chem C 112:10462
21. Ayta WEF, Silva VA, Dantas NO (2010) J Lumin 130:1032
22. Moustafa YM, Doweidar H, El-Damrawi G (1994) Phys Chem Glasses 35:104
23. Moustafa YM, El-Egili K (1998) J Non Cryst Solids 240:144
24. Kamitsos EI, Patsis AP, Karakassides MA, Chryssikos GD (1990) J Non Cryst Solids 126:52
25. Kamitsos EI, Karakassides MA, Chryssikos GD (1987) J Phys Chem 91:1073
26. Kamitsos EI, Karakassides MA, Chryssikos GD (1987) Phys Chem Glasses 28:203
27. Doweidar H, Saddeek YB (2009) J Non Cryst Solids 355:348
28. Doweidar H, Saddeek YB (2010) J Non Cryst Solids 356:1452
29. Doweidar H, El-Egili K, El-Damrawi G, Ramadan RM (2008) Phys Chem Glasses 4(9):271
30. Yiannopoulos YD, Chryssikos GD, Kamitsos EI (2001) Phys Chem Glasses 42:164
31. Ohtori N, Takase K, Akiyama I, Suzuki Y, Handa K, Sakai I, Iwadate Y, Funukaga T, Umesaki N (2001) J Non Cryst Solids 293–295:136
32. Kamitsos EI, Karakassides MA (1988) Solid State Ionics 28–30:783
33. Web Elements Periodic Table of Elements. http://www.webelements.com
34. Doweidar H (2009) J Non Cryst Solids 355:577
35. Shaw RR, Uhlmann DR (1969) J Non Cryst Solids 1:474
36. Doweidar H, Oraby AH (1997) Phys Chem Glasses 38:69
37. Doweidar H, Moustafa YM, Abd El-Maksoud S, Silim H (2001) Mater Sci Eng A 301:207
38. Leide DR (ed) (2005) CRC Handbook of Chemistry and Physics, 85th edn. CRC Press, Boca Raton
39. Watanabe T, Hayashi M, Hayashi S, Fukuyama H, Nagata K (2004) VII International Conference on Molten Slags Fluxes and Salts, The South African Institute of Mining and Metallurgy, 699
40. Brauer DS, Karpukhina N, Lawb RV, Hill RG (2009) J Mater Chem 19:5629
41. Boden N, Kahol PK, Mee A, Mortimer M, Peterson GN (1983) J Magn Reson 54:419
42. Brauer DS, Al-Noaman A, Hill RG, Doweidar H (2011) Mater Chem Phys 130:121
43. Kittel C (1996) Introduction to Solid State Physics, 7th edn. Wiley, New York
44. Jain H, Downing HL, Peterson NL (1984) J Non Cryst Solids 64:335